Anomalous Features in the Potential Energy Landscape of a Waterlike Monatomic Model with Liquid and Glass Polymorphism

Gang Sun, Limei Xu, and Nicolas Giovambattista

Anomalous features in the potential energy landscape of a water-like monatomic model with liquid and glass polymorphism

Gang Sun[1,2], Limei Xu[1,3],* and Nicolas Giovambattista[4,5]†

[1] International Center for Quantum Materials, School of Physics,
Peking University, Beijing 100871, China
[2] School of Chemistry, University of Sydney,
Sydney, NSW, Australia
[3] Collaborative Innovation Center of Quantum Matter, Beijing, China
[4] Department of Physics,
Brooklyn College of the City University of New York,
Brooklyn, New York 11210, United States
[5] Ph.D. Programs in Chemistry and Physics,
The Graduate Center of the City University of New York,
New York, NY 10016, United States
(Dated: December 13, 2017)

We study the potential energy landscape (PEL) of a water-like monatomic liquid that exhibits a liquid-liquid phase transition (LLPT) and glass-glass transformation (GGT). We identify two anomalous features of the PEL that give origin to both phenomena. Specifically, during the pressure-induced LLPT and GGT, (i) the inherent structures (IS) energy becomes a concave function of volume, and (ii) the IS pressure exhibits a van der-Waals-like loop. We argue that features (i) and (ii) imply that the GGT is a (non-equilibrium) first-order phase transition, analogous to the LLPT. Interestingly, contrary to the case of ST2 water, (a) we do not find separate PEL megabasins for LDA/LDL and HDL/HDA; and (b) features (i)(ii) persist at temperature well above the LLPT.

Glass polymorphism is the ability of a substance to exist in more than one amorphous solid state. Examples include substances that are very important in scientific and technological applications, such as water [1–9], silicon [10, 11], germanium [12], and yttrium oxide-aluminum oxide melts [13]. In these substances, a low-density and a high-density amorphous solid (LDA and HDA) can be identified and the transformation between LDA and HDA is sharp, reminiscent of a first-order phase transition between equilibrium states. A scenario commonly used to interpret this phenomenon is provided by the liquid-liquid phase transition (LLPT) hypothesis, originally proposed for the case of water [14]. In this scenario [15–17], there are two different liquid states, low-density and high-density liquid (LDL and HDL), which are connected thermodynamically with LDA and HDA, respectively, e.g., by isobaric cooling/heating. In particular, LDL and HDL are separated by a liquid-liquid first-order phase transition line that ends at a liquid-liquid critical point (LLCP). In this scenario, the LLPT, extended into the glass domain, becomes a 'first-order phase transition' between LDA and HDA.

The possibility that a substance can exhibit a first-order phase transition between two 'out-of-equilibrium (amorphous solid) states' (LDA and HDA) remains as a challenging concept in condensed matter physics. This is because there is no well-established explanation of glass polymorphism in the context of thermodynamic and statistical mechanics. How do we extend, if possible, the tools from *equilibrium* thermodynamics/statistical mechanics to discriminate among a sharp-but-continuous LDA-HDA transformations, and a LDA-HDA true first-order phase transition? A theoretical framework that describes both the LLPT and LDA-HDA transformation and that, in particular, can incorporate phenomena inherent to the glass state, such as annealing and glass preparation effects, is not available. In a recent work [18], this question was addressed for the case of *ST2 water* using the potential energy landscape (PEL) formalism; however, it is not evident how general the conclusions of Ref. [18] are. For a system of N atoms, the PEL is the hypersurface in $(3N + 1)$-dimensional space defined by the potential energy of the system as function of the atom coordinates, $V(\vec{r}_1, \vec{r}_2, ..., \vec{r}_N)$ [19]. At any given time t, the system is represented by a single point on the PEL given by the atom coordinates at t. Hence, as the atom coordinates change with time, the system moves, describing a trajectory on the PEL. In the high-temperature liquid state, the system can 'visit' large regions of the PEL while, at low temperatures, the system is constrained to move within more localized regions of the PEL. Upon further cooling, in the glass state, ergodicity is broken and the system can only explore specific basins of the PEL. The minima of the PEL basins are called inherent structures (IS). A complete theory for low-temperature liquids based on the topography of the PEL has been developed. This theory allows one to express the free energy of liquids in terms of the IS energy E_{IS} (basin depth), Hessian of the PEL at the IS (basin curvature), and distributions of IS in the PEL (density of IS states) [20].

In this work, we show that the PEL formalism, a theoretical framework within statistical mechanics, provides a simple understanding of the LDA-HDA transformation. Specifically, we employ computer simulations to study

the PEL of the Fermi-Jagla (FJ) model, a water-like monatomic system with isotropic two-scale pair interactions [21–24]; see inset of Fig. 1(a) and Refs. [21, 22]. In the liquid state, this model exhibits a LLPT ending at a LLCP [22] [see Fig. S1 of the supplementary material (SM)] and a first-order-like phase transition between LDA and HDA forms [22, 25, 26]. We follow the same procedure used in Refs. [18, 27] for the case of ST2 and SPC/E water and explore whether the PEL description of water polymorphism is general, e.g., independent of the presence of hydrogen-bond interactions. We find that similar to the case of ST2 water [18, 28], albeit some differences exist, the LLPT and LDA-HDA transformation are accompanied by anomalous behavior in specific properties of the PEL.

We perform molecular dynamics (MD) simulations over a wide range of volumes and temperatures (see SM for computer simulation details). In order to calculate the PEL properties of the system in the liquid and glass states, we calculate the IS of selected configurations by minimization of the potential energy using the conjugate gradient algorithm [21, 29]. For the liquid at a given (v, T) state, we select 100 independent configurations; for the LDA-HDA transformation, we employ ten independent trajectories and show the PEL properties of all trajectories at selected pressures, without averaging.

We focus on the evolution of the IS energy $E_{IS}(v)$, IS pressure $P_{IS}(v)$, and shape function $\mathcal{S}_{IS}(v)$ along isotherms. The virial expression at the IS sampled by the system defines $P_{IS}(v)$, and the shape function $\mathcal{S}_{IS}$ quantifies the curvature of the basins at the corresponding IS,

$$\mathcal{S}_{IS} = \frac{1}{N} \left\langle \sum_{i=0}^{3N} \ln \left(\frac{\omega_i}{\omega_0} \right) \right\rangle \qquad (1)$$

Here, $\langle ... \rangle$ indicates average over the IS sampled by the system at a given (v, T) and $\{\omega_i^2\}_{i=1...3N}$ are the eigenvalues of the Hessian matrix at these IS. ω_0 is a constant needed to make the argument of the ln function adimensional [20]; in this work, $\omega_0 = 1$ (in reduced units). These quantities are fundamental properties of the PEL; for example, for equilibrium low-temperature liquids, $E_{IS}(v)$, $P_{IS}(v)$, and $\mathcal{S}_{IS}(v)$ define the total energy and pressure of the system at a given T [20].

$E_{IS}(v)$, $P_{IS}(v)$, and $\mathcal{S}_{IS}(v)$ are shown in Fig. 1 for different *liquid* isotherms, above and below the LLCP (empty symbols), and during the pressure-induced LDA-HDA transformation of ten independent runs at $T = 0.01$ (solid symbols). We note that for a system of soft-spheres, a model liquid with no LLPT, one finds that at low temperatures $E_{IS}(v)$, $P_{IS}(v)$, $\mathcal{S}_{IS}(v)$, and their first derivatives with respect to volume, are all monotonic decaying functions of v (see Ref. [20], Sec. 7.2). Instead, for the FJ liquid across the LLPT and LDA-HDA transformation, (i) $E_{IS}(v)$ shows an anomalous region with negative curvature, while (ii) $P_{IS}(v)$ exhibits a van der Waals-like loop. The behavior of $\mathcal{S}_{IS}(v)$ is rather common, with no apparent feature that may be indicative of a LLPT; the basins become smoothly and increasingly thinner during compression. Fig. 1 strongly suggests that features (i) and (ii) are the PEL characteristics responsible to the LLPT and glass-glass first-order-like phase transition.

Both features (i) and (ii) can be explained within the PEL formalism. Specifically, in the PEL approach, a liquid in equilibrium can be considered to be composed of two subsystems [20], a subsystem that depends solely on the IS energy and distribution of IS in the PEL (*IS*-subsystem), and a subsystem that depends solely on the vibrational motion of the system within the basins of the PEL (*vib*-subsystem). The subsystems are characterized by Helmholtz free energies F_{IS} and F_{vib}, and the free energy of the liquid can be expressed as

$$F = F_{IS} + F_{vib} \qquad (2)$$

A similar additive expression can be written for the total energy of the liquid, $E = E_{IS} + E_{vib}$. It follows that within the PEL approach, $F = E_{IS} + E_{vib} - TS$. By definition, $E_{vib}(T)$ must be an increasing function of T; indeed, in the harmonic approximation of the PEL, $E_{vib} = 3Nk_BT$ [30]. Accordingly, at sufficiently low temperatures, $F(v) \approx E_{IS}(v)$. The stability condition of thermodynamics requires $F(v)$ to exhibit a region of concavity during a first-order phase transition at constant N and T [31]. Hence, for a liquid with a low-temperature LLPT, the curvature of $E_{IS}(v)$ along isotherms ($T < T_c$) must also exhibit a concavity region. These arguments explain feature (i) in Fig. 1(b). To confirm this explanation, we calculate the term $-TS/N$ and find that this quantity barely varies during the LLPT and changes within a range of 0.05 (see SM). We also confirm that $E_{vib}(v)$ does not exhibit any concavity region within the LLPT ($2.4 < v < 3.4$); see Fig. 2(a). Since only $E_{IS}(v)$ can be responsible for the concavity in $F(v)$, the LLPT can only be originated by the *IS*-subsystem, i.e., by structural changes in the liquid.

A similar argument can be used to explain feature (ii) in Fig. 1(a). Specifically, it follows from Eq. 2 that $P = P_{IS} + P_{vib}$, where P_{vib} is the pressure contribution from the *vib*-subsystem. We find that, at constant v, P_{vib} is a linear function of T at low temperature ($T < 0.2$). Indeed, in the harmonic approximation of the PEL, $P_{vib} = -Nk_BT \left(\frac{\partial \mathcal{S}_{IS}}{\partial V} \right)_{Evib,N}$ and $E_{vib} = 3Nk_BT$ implying that, for T-independent basin curvatures, $P_{vib} \propto T$ (constant v). It follows that for a liquid with a first-order phase transition at low temperature, $P(v) \approx P_{IS}(v)$ along isotherms and hence, a van der Walls loop in $P(v)$ should be accompanied by a van der Waals loop in $P_{IS}(v)$. These arguments explain feature (ii) in Fig. 1(a). We confirm that $P_{vib}(v)$ does not exhibit any van der Waals-like loops during the LLPT

region; see Fig. 2(c) Therefore, as concluded in the previous paragraph, the LLPT is due to anomalous changes in the IS-subsystem.

We note that the arguments presented above are valid for an equilibrium (or metastable) liquid at low temperatures. However, similar arguments may be applied to the case of the LDA-HDA transformations *if* Eq. 2 can be justified for the glass state. This is plausible if one introduces an out-of-equilibrium configurational entropy, which would depend on the glass preparation process [18]. Consistent with this argument, our (out-of-equilibrium) simulations during the LDA-HDA transformations show similar results to those reported for the LLPT. This is shown in Figs. 1(a)-(c) where we include $E_{IS}(v)$, $P_{IS}(v)$, and $\mathcal{S}_{IS}(v)$ during the pressure-induced LDA-HDA transformation at $T = 0.01$.

Next, we compare the PEL of ST2 water and FJ model. This is relevant since although both systems exhibit a LLPT and a LDA-HDA first-order-like phase transition, the ST2 model is full-atomistic with molecules forming hydrogen bonds in a local tetrahedral arrangements while, in the FJ model, interactions are isotropic with atoms arranged in non-tetrahedral structures. Accordingly, one may expect that the topology of the PEL of these two models are different. Hence, it is natural to ask whether the same anomalous features of the PEL are present in both systems during the corresponding LLPT and LDA-HDA transformation. If so, these phenomena would have a common explanation within the PEL formalism, independently of molecular details. In addition, we will test whether the conditions in Refs. [18, 28] to classify the LDA-HDA transformation as a first order phase transitions also apply to the sharp (first-order-like) LDA-HDA transformation of the FJ liquid.

In the case of ST2 water, $E_{IS}(v)$ and $P_{IS}(v)$ also exhibit the features (i) and (ii) described above during the LDA/LDL-HDA/HDL transformations [18]. However, in ST2 water there is also a sudden, non-monotonic change in the basins curvature, as quantified by $\mathcal{S}_{IS}(v)$, which is not found in the FJ liquid. The results from the PEL study of ST2 water and FJ liquid (and the justifications presented above) suggest that the properties of the PEL responsible for the LLPT are features (i) and (ii) mentioned above, while changes in the shape of the basins across the LLPT play no role. In particular, these studies strongly indicate that for an LDA-HDA transformation to be considered a first-order phase transition, $E_{IS}(v)$ and $P_{IS}(v)$ must exhibit features (i) and (ii) [28].

In the case of ST2 water, during the LLPT and LDA-HDA transformation, $E_{IS}(v)$ develops a maximum, consistent with the view that the PEL has two megabasins [32–36], one for LDL/LDA and another for HDL/HDA. As show in Fig. 1(b), this is not the case for the FJ liquid. Yet, the PEL can still be divided into two *regions*, one associated with LDL/LDA and another with HDL/HDA but it is the curvature of $E_{IS}(v)$ that sets the boundaries between these regions.

We note a very peculiar difference in the PEL of ST2 water and FJ model. In the case of ST2 water, features (i) and (ii) vanish at approximately $T > T_c$. However, in the FJ liquid, features (i) and (ii) can be found even at $T > T_c$. This is important since it means that the concavity of $E_{IS}(v)$ and the van der Waals loop of $P_{IS}(v)$ are *necessary but not sufficient* features of the PEL for a system to exhibit liquid and/or glass polymorphism. Specifically, at $T > T_c$, the concavity of $E_{IS}(v)$ may remain but it may be compensated by the behavior of $E_{vib}(v)$ leading to no concavity in $E(v)$ and hence, no concavity in $F(v)$ at high temperatures. In addition, entropic contribution to $F(v)$ may remove any concavity arising from $E(v)$. Similarly, the van der Waals loop of $P_{IS}(v)$ at $T > T_c$ is suppressed by the behavior of $P_{vib}(v)$, leading to no van der Waals loop in $P(v)$.

The anomalous behavior of $E_{IS}(v)$ and $P_{IS}(v)$ at $T > T_c$ in the FJ liquid is also of practical relevance. Specifically, features (i) and (ii), indicative of the LLPT at low temperatures, can be detected at temperatures as high as $T \approx 5\,T_c$. We note that other quantities, such as the potential energy $U(v)$, can also be used as an indicator of a LLPT at low temperature [37–39]; see SM.

An interesting observation for the case of ST2 water involves the path followed by the liquid and glass in the PEL. Specifically, MD simulations show that, during the pressure-induced LDL-HDL and LDA-HDA transformations, the system moves between the LDL/LDA and HDL/HDA regions/basins of the PEL [18, 27]. Yet, the paths followed by the liquid and the glass are different. We confirm that this scenario also holds for the FJ liquid. Fig. 3(a) and 3(b) show $P_{IS}(E_{IS})$ and $\mathcal{S}_{IS}(E_{IS})$ for the liquid (empty symbols) and glass (solid symbols). The non-overlapping path of the LDA-HDA transformation and the equilibrium liquid in Fig. 3(a) and 3(b) implies that the amorphous solid explores basins of the PEL that are not sampled by the liquid in equilibrium (including the IS sampled during the LLPT [18]).

In summary, as found in ST2 water, the LLPT and LDA-HDA transformation in the FJ model can be identified with two anomalous properties of the PEL, a concavity region in $E_{IS}(v)$ and a van der Waals-like loop in $P_{IS}(v)$ (at constant temperature). Although two regions of the PEL can be associated to LDA/LDA and HDL/HDA, these domains are not distinct PEL megabasins (two megabasins were identified in the PEL of ST2 water [18, 28]). Finally, contrary to ST2 water, the anomalies in the PEL of the FJ liquid remain at temperatures well above the LLCP temperature.

ACKNOWLEDGMENTS

———————

* limei.xu@pku.edu.cn
† ngiovambattista@brooklyn.cuny.edu

[1] O. Mishima, L. D.Calvert, and E. Whalley, Nature **314**, 76 (1985).

[2] K. Winkel, M. Bauer, E. Mayer *et al.*, Phys.: Condens. Matter **20**, 494212 (2008).

[3] T. Loerting, W. Schustereder, K. Winkel *et al.*, Phys. Rev. Lett. **96**, 025702 (2006).

[4] O. Mishima, Phys. Rev. Lett. **85**, 334 (2000).

[5] O. Mishima, J. Chem. Phys. **133**, 144503 (2010).

[6] O. Andersson and A. Inaba, Phys. Rev. B **74**, 184201 (2006).

[7] S. Klotz, Th. Strässle, R. J. Nelmes, J. S. Loveday, G. Hamel, G. Rousse, B. Canny, J. C. Chervin, and A. M. Saitta, Phys. Rev. Lett. **94**, 025506 (2005).

[8] M. M. Koza, H. Schober, H. E. Fischer, T. Hansen, and F. Fujara, J. Phys.: Condens. Matter **15**, 321 (2003).

[9] F. Franks, *Water: A Matrix of Life*, (2nd Ed, the Royal Society of Chemistry, UK, 2000).

[10] P. F. McMillan, M. Wilson, D. Daisenberger, and D. Machon, Nat. Mater. 4, 680 (2005).

[11] M. Grimsditch, Phys. Rev. Lett. **52**, 2379 (1984).

[12] M. H. Bhat, V. Molinero, E. Soignard, V. C. Solomon, S. Sastry, J. L. Yarger, and C. A. Angell, Nature **448**, 787 (2007).

[13] M. C. Wilding and P. F. McMillan, J. Non-Crystalline Solids **293-295**, 357 (2001).

[14] P. H. Poole, F. Sciortino, U. Essmann *et al.*, Nature **360**, 324 (1992).

[15] O. Mishima and H. E. Stanley, Nature **396**, 329 (1998).

[16] P. G. Debenedetti, J. Phys.: Condens. Matter **15**, R1669 (2003).

[17] P. Gallo *et al.*, Chem. Rev. **116**, 7463 (2016).

[18] N. Giovambattista, F. Sciortino, F. W. Starr, and P. H. Poole, J. Chem. Phys. **145**, 224501 (2016).

[19] F. H. Stillinger, Science **267**, 1935 (1995).

[20] F. Sciortino, J. Stat. Mech. **2005**, P05015 (2005).

[21] G. Sun, L. Xu, and N. Giovambattista, J. Chem. Phys. **146**, 014503 (2017)

[22] J. Y. Abraham, S. V. Buldyrev, and N. Giovambattista, J. Phys. Chem. B **115**, 14229 (2011).

[23] A. Skibinsky, S. V. Buldyrev, G. Franzese, G. Malescio, and H. E. Stanley, Phys. Rev. E **69**, 061206 (2004).

[24] G. Franzese, G. Malescio, A. Skibinsky, S. V. Buldyrev, and H. E. Stanley, Nature **409**, 692 (2001).

[25] S. Reisman and N. Giovambattista, J. Chem. Phys. **138**, 064509 (2013).

[26] A. Gordon and N. Giovambattista, Phys. Rev. Lett. **112**, 145701 (2014).

[27] N. Giovambattista, H. E. Stanley, and F. Sciortino, Phys. Rev. Lett. **91**, 115504 (2003).

[28] N. Giovambattistam, F. W. Starr, and P. H. Poole, J. Chem. Phys. **147**, 044501 (2017).

[29] W. H. Press, B. P. Flannery, A. A. Teukolsky et al., *Numerical Recipes: The Art of Scientific Computing* (Cambridge: Cambridge University, 1986).

[30] I. Saika-Voivod, F. Sciortino, and P. H. Poole1, Phys. Rev. E **69**, 041503 (2004).

[31] H. B. Callen, *Thermodynamics and an Introduction to Thermostatistics* (John Wiley & Sons, Inc., New York, 1985).

[32] B. Doliwa and A. Heuer, Phys. Rev. E **67**, 030501(R) (2003).

[33] G. A. Appignanesi, J. A. Rodriguez Fris, R. A. Montani, and W. Kob, Phys. Rev. Lett. **96**, 057801 (2006).

[34] T. Loerting *et al.*, Phys. Chem. Chem. Phys. **13**, 8783 (2011).

[35] O. Mishima, Nature **384**, 546 (1996).

[36] D. Machon, F. Meersman, M. C. Wilding, M. Wilson, and P. F. McMillan, Prog. Mat. Sci. **61**, 216 (2014).

[37] P. H. Poole, S. R. Becker, F. Sciortino, and F. W. Starr, J. Phys. Chem. B **115**, 14176 (2011).

[38] F. Sciortino, P. H. Poole, U. Essmann, H. E. Stanley, Phys. Rev. E **55**, 727 (1997).

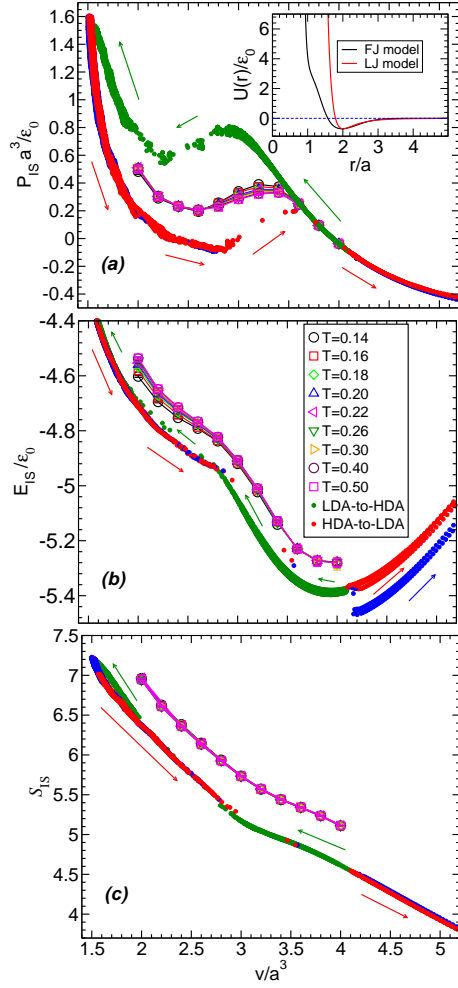[39] A. Scala, G. W. Starr, E. La Nave, H. E. Stanley, F. Sciortino, Phys. Rev. E **62**, 8016 (2000).

FIG. 1. (a) Pressure $P_{IS}(v)$, (b) energy per particle $E_{IS}(T)$, and (c) basin shape function $\mathcal{S}_{IS}(v)$ of the IS sampled by the equilibrium liquid at constant temperatures (open symbols). Also included are $P_{IS}(v)$, $E_{IS}(v)$, and $\mathcal{S}_{IS}(v)$ during the isothermal compression of ten independent LDA configurations at $T = 0.01$ (solid dark-green circles) and the corresponding decompression of the resulting HDA from $P = 1.5$ (solid blue and red circles; blue circles represent the two trajectories that crystallize rapidly after LDA is formed). In (b) and (c), $E_{IS}(v)$ and $\mathcal{S}_{IS}(v)$ for the LDA-HDA transformations are shifted by $\Delta E_{IS} = -0.1$ and $\Delta \mathcal{S}_{IS}(v) = -0.5$. The inset in (a) shows the FJ pair interaction potential $U(r)$ characterized by a hard-core radius $r \approx a$, a core-softened part at $a \leq r \leq b \approx 2a$, and a weak attractive part; a Lennard-Jones pair potential with same minimum depth and location is included for comparison.
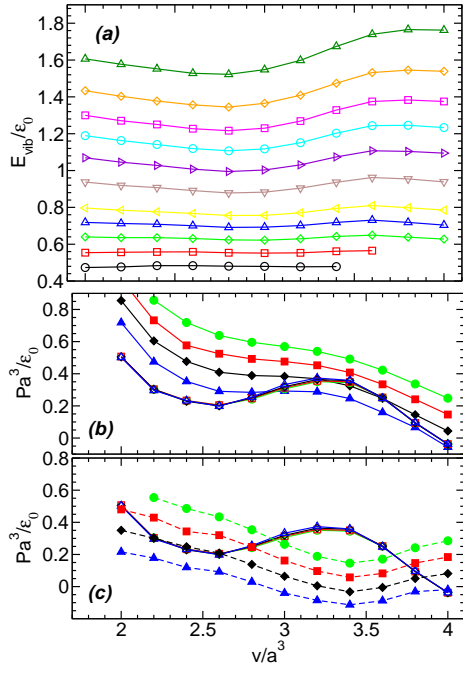
FIG. 2. (a) Vibrational energy $E_{vib}(v)$ as function of volume for different isotherms (bottom to top: $T = 0.14, 0.16, 0.18, 0.20, 0.22, 0.26, 0.30, 0.34, 0.38, 0.43, 0.50$). $E_{vib}(v)$ is a weak, non-monotonic function of v and exhibits a minimum at $v = 2.8 - 3.0$ for all temperatures. (b) Pressure $P(v)$ (solid symbols) and IS pressure $P_{IS}(v)$ (empty symbols) at $T = 0.16$ (up-triangles), $T = T_c = 0.18$ (diamonds), $T = 0.20$ (squares), and $T = 0.22$ (circles). (c) Vibrational pressure $P_{vib}(v)$ compared to $P_{IS}(v)$ for the same temperatures included in (b). In (b) and (c), isotherms of $P(v)$ and $P_{vib}(v)$ are shifted by $\Delta P = -0.1, 0.0, 0.1, 0.2$ for $T = 0.16, 0.18, 0.20, 0.22$ respectively. The volumes where the liquid is unstable correspond to $(\partial P/\partial v)_T > 0$. At these volumes (approximately $2.4 \leq v \leq 3.4$), $(\partial P_{IS}/\partial v)_T > 0$ but $(\partial P_{vib}/\partial v)_T < 0$, and $E_{vib}(v)$ has a positive curvature.
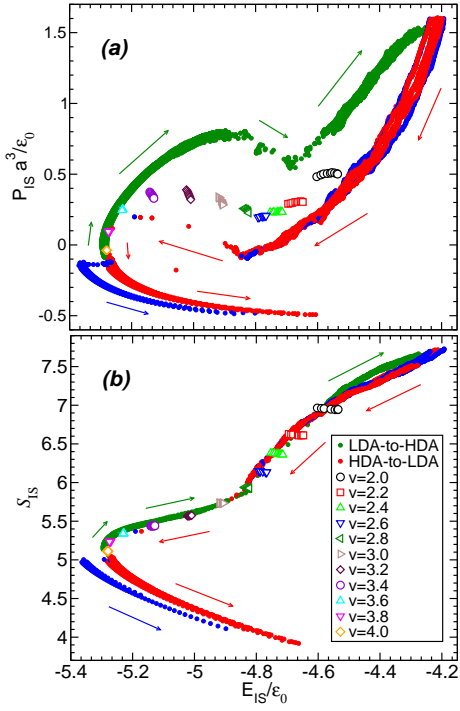
FIG. 3. (a) $P_{IS}(E_{IS})$ and (b) $\mathcal{S}_{IS}(E_{IS})$ during the LDA-to-HDA (solid dark-green circles) and HDA-to-LDA transformation (solid red and blue circles; blue circles represent the two trajectories that crystallized) at $T = 0.01$. The corresponding $P_{IS}(E_{IS})$ and $\mathcal{S}_{IS}(E_{IS})$ for the equilibrium liquid is also included (open symbols). During the LDA-HDA transformations, the system samples IS never explored by the equilibrium liquid. Data is taken from Fig. 1.